Available online at www.sciencedirect.com
SCIENCE DIRECT®
Journal of Nuclear Materials 346 (2005) 194–207
journal of nuclear materials
www.elsevier.com/locate/jnucmat

The effect of composition on the leaching of three nuclear waste glasses: R7T7, AVM and VRZ

Pierre Frugier [a,*], Christelle Martin [a], Isabelle Ribet [a], Thierry Advocat [b], Stéphane Gin [a]

[a] CEA Valrhô Marcoule, DEN/VRH/DTCD/SECM/LCLT, BP 17171, 30207 Bagnols-sur-Cèze cedex, France
[b] CEA Valrhô Marcoule, DEN/VRH/DTCD/SCDV/LMPA, BP 17171, 30207 Bagnols-sur-Cèze cedex, France

Received 10 October 2002; accepted 21 June 2005

Abstract

The influence of composition variations on long-term glass behavior was investigated for three nuclear glass composition domains: the French SON 68 (R7T7-type) glass, the Na–Mg borosilicate AVM glass and the aluminosilicate VRZ glass defined as part of the investigation of new containment matrices based on zirconolite ($CaZrTi_2O_7$). The initial alteration rates for glasses from different domains are comparable. Conversely, the alteration kinetics at advanced stages of reaction progress are very different, with decreases in the rates corresponding to different kinetic profiles, i.e. altered thickness versus time. The altered glass thickness can depend on the initial alteration rate and especially on the decrease in the rate, or it can be determined by the high residual alteration rate. The variation of the alteration rates over time appears to be related to the alteration film that forms on the surface of the material in particular the presence of any secondary crystalline phases. For AVM glass, the high residual rate is attributed to phyllosilicate phases rich in magnesium.

1. Introduction

Long-term behavior studies concerning French nuclear glass are generally carried out on a reference glass such as SON68 for the R7T7 domain. However, the influence of the composition must be assessed to extend predictions based on the reference glass to an industrially specified composition domain.

The influence of the composition on the initial alteration rate has already been extensively covered in the literature [1–4], but the influence of the composition on the alteration rate at advanced stages of reaction progress has not often been considered. The second parameter is more representative of disposal conditions, however, and is indicative of the predominant long-term alteration mechanisms. Leach tests were therefore carried out to estimate not only the initial rate but also the rate at advanced stages of reaction progress.

The observed slowdown of the alteration rate of nuclear glasses has long been attributed to the effect of chemical affinity, i.e. the diminishing difference between the chemical potential of the solution (which increases as the solution becomes saturated) and the constant chemical potential of the glass [5–7]. This theory has been

* Corresponding author. Tel.: +33 4 66 79 76 94; fax: 33 4 66 79 66 20.
E-mail address: pierre.frugier@cea.fr (P. Frugier).

0022-3115/$ - see front matter © 2005 Elsevier B.V. All rights reserved.
doi:10.1016/j.jnucmat.2005.06.023

called into question, however, [8–10] and the mechanism currently taken into consideration by the CEA is the development of a protective gel forming a diffusion barrier for reactive species. According to this theory, the kinetics are limited only by the transport of reactive species (coming from the glass dissolution) through the gel layer [11,12].

This gel is the result of an in situ rearrangement of hydrated species. The formation of a protective gel implies the presence of silicon together with other elements (Al, Zr, Ca, etc.) at the reaction interface. The incorporation of insoluble elements in the glass does not always result in the formation of protective gels, however. Conversely, the alkaline-earths (calcium in particular) favor the development of protective gels. During studies of simplified glasses with the same elemental ratios as R7T7 glass, it has been observed that the simultaneous presence of Al and Ca or of Zr and Ca deeply modifies the protective effect of the gel layer, what leads to a slowdown of the alteration rate more or less rapid and important [8,13,14]. Silicon retention within the gel is also considered to be one of the parameters affecting the protective properties of the gel layer. It is currently considered that the higher the retention factor f_{Si}, the more protective the gel [10]. The alteration film does not consist only of a potentially protective amorphous gel: the alteration of most complex glass compositions leads to the precipitation of 'secondary' phases from solution. They crystallize and are not considered to have protective properties: some of these phases are thought to sustain glass alteration, or even to induce renewed alteration by consuming elements from the gel layer during their crystallization [15]. The gels formed by R7T7 glass alteration at temperatures below 150 °C are mainly amorphous: the only crystalline phases detected are smectitic phyllosilicates [16,17]. Until very recently, no studies of R7T7 glass alteration had revealed any signs of a resumption of alteration. Renewed alteration was observed only during R7T7 glass alteration studies at very high imposed pH values. The resumption of alteration at pH > 11 was related to the appearance of a zeolitic crystalline phase [14].

The alteration films that formed on the surface of glasses from the different domains were therefore characterized to observe the link between the nature of the film and the kinetic profile of each glass.

2. Experimental

2.1. Composition domains

Three composition domains were studied. The R7T7 domain is the specification domain for all glasses currently used for the containment of light water reaction (LWR) fission product solutions produced by reprocessing UOX1 fuel with burnup values ranging from 30 to 45 GW d/t. They are produced industrially by COGEMA in the R7 and T7 vitrification units at La Hague [18]. The AVM domain corresponds to the glass compositions produced in the Marcoule vitrification facility for various types of fuel, mainly from gas–graphite reactors.

The VRZ domain has been defined for the investigation of a new containment material under consideration for specific conditioning of plutonium or the minor actinides: the zirconolite glass–ceramic matrix. It is composed of zirconolite crystals ($CaZrTi_2O_7$) dispersed in a residual glass phase. The actinides (or neodymium which is used as an actinide surrogate) are distributed throughout the zirconolite crystals and the vitreous phase. Since zirconolite alteration is extremely limited, actinide release during the glass–ceramic alteration is mainly attributable to alteration of the residual glass. Consequently, the aim of glass–ceramic material development is to put as many actinides as possible into the crystalline phase and study of its leaching implies the study of the alteration of the residual glass (VRZ glass) [19,20].

Zirconolite glass–ceramic is produced by melting an oxide mixture (parent glass) and submitting it to a heat treatment that directly determines the degree of crystallization, and thus the composition of the residual vitreous phase. The limits of the composition domain were defined from these variable degrees of crystallization. They take into account possible variations in the parent glass composition too. The zirconium and titanium content of the parent glass could be increased in the future to favor zirconolite crystallization and thus increase the neodymium fraction in the zirconolite [21,22].

AVM and R7T7 glasses have several common constituents. AVM glass differs from R7T7 glass mainly by a lower silicon concentration, a higher Al_2O_3 concentration, the presence of MgO and the virtual absence of CaO. The residual zirconolite glass differs significantly from AVM and R7T7 glass in particular by its low B_2O_3 concentration, the absence of alkalis, its high CaO and Nd_2O_3 concentrations, and the presence of TiO_2.

Table 1 summarizes the three glass domains studied. Only the influence of the major constituents (variables in Table 1) was investigated. The constituents with minor variations were not taken into account: their effects were assumed to be limited and masked by the effects of the major constituents.

2.2. Experimentation plan

Having specified the extent of the composition domains, the problem was to determine which glasses

Table 1
Description of the three composition domains: variation ranges (wt%) and relational constraints

	R7T7	AVM	VRZ
SiO_2	42.40–51.68	38.5–46	40.8–55.6
B_2O_3	12.40–16.50	16–19.5	1.0
Na_2O	8.10–11.00	5–18.8	
Al_2O_3	3.60–6.60	9–12.5	9–13.7
CaO	4.0	0.2	19.7–24.6
Nd_2O_3	0.5–2.6	0.1–0.9	1–6.5
ZrO_2	2.0–4.9	0.1–1.0	2–12
TiO_2			6.2–15.5
MgO		2.5–7.5	
$Fe_2O_3 + NiO + Cr_2O_3$	0.4–5.6	2.8	
F		0–1.8	
P_2O_5	0.5	0–1.7	
$FP + Act + MoO_3 + Gd_2O_3 + Ag_2O$	3.53–17.95	0–10.2	
Fines	0.01–6.85		
ZnO	2.5		
Li_2O	2.0	0.4	
SO_3		0.1	
Cl		0.1	
CdO		0.5	
Relational constraints	$3.01 < SiO_2/B_2O_3 < 3.47$	Frit constant	$TiO_2–ZrO_2 < 8$
	$7.0 < FP + Act + Fines < 18.0$	$MgO + Al_2O_3 < 18.5$	$ZrO_2–TiO_2 < 1$
	$FP + Act > Fines$	$Al_2O_3 < 3*[(Na_2O + Li_2O)–0.278SiO_2]$	
	$SiO_2 + B_2O_3 + Al_2O_3 > 60.0$	$FP + Act + MoO_3 + Gd_2O_3 + Ag_2O > 0.5MgO$	
	$Fe_2O_3/NiO = 7.09$		
	$Fe_2O_3/Cr_2O_3 = 5.73$		

Oxide breakdown (wt%) compared with reference glass

wt%	R7T7		AVM
	FP + Act	Fines	FP + Act + ⋯
SrO	0.34		0.21
ZrO_2	1.70	0.47	0.96
MnO_2	0.30	0.08	0.31
Cs_2O	1.10		0.71
BaO	0.61		0.34
Y_2O_3	0.20		0.12
La_2O_3	0.92		0.56
Ce_2O_3	0.95		0.60
Nd_2O_3	1.63		0.93
Pr_2O_3	0.45		0.28
SnO_2	0.02		0.02
Sb_2O_3	0.00		0.01
TeO_2	0.23		0.14
ThO_2	0.31		0.11
UO_2	0.05	0.01	0.70
MoO_3	1.36	0.39	0.75
Ag_2O	0.03		0.10
RuO_2	0.63	0.36	
Rh	0.12	0.05	
Pd	0.33	0.10	
CdO	0.03		
Gd_2O_3			0.60

'Fines' include platinum-group metals and metallic particles, FP refers to fission products.

would best describe them, considering a limited number of tests. The experimentation plan [23,24] was therefore applied to this mixture problem to describe the variations of the alteration rates (initial alteration rate r_0 and the residual alteration rate r_f) on each composition domain. The methodology consists to postulate a mathematic model that allows to calculate the alteration rate of a glass according to its composition. By limiting the mixing model to the constituents significantly affecting the alteration rate, it considerably optimizes the number of tests that must be carried out for each domain. The models postulated here are first-order models enriched with second-degree terms to take into account the interactions among the major constituents:

$$\begin{aligned}
r(\mathrm{R7T7}) &= a_1\mathrm{SiO_2} + a_2\mathrm{B_2O_3} + a_3\mathrm{Na_2O} + a_4\mathrm{Al_2O_3} + a_5\mathrm{Fe_2O_3} + a_6\mathrm{Fines} + a_7\mathrm{FP} + a_{12}\mathrm{SiO_2} * \mathrm{B_2O_3} \\
&\quad + a_{13}\mathrm{SiO_2} * \mathrm{Na_2O} + a_{23}\mathrm{B_2O_3} * \mathrm{Na_2O} + a_{14}\mathrm{SiO_2} * \mathrm{Al_2O_3} + a_{34}\mathrm{Na_2O} * \mathrm{Al_2O_3} + a_{15}\mathrm{SiO_2} * \mathrm{Fe_2O_3}. \\
&\quad + a_{16}\mathrm{SiO_2} * \mathrm{Fines} + a_{17}\mathrm{SiO_2} * \mathrm{FP} \\
r(\mathrm{AVM}) &= b_1\mathrm{SiO_2} + b_2\mathrm{B_2O_3} + b_3\mathrm{Na_2O} + b_4\mathrm{Al_2O_3} + b_5\mathrm{MgO} + b_6\mathrm{Fines} + b_7\mathrm{FP} + b_{12}\mathrm{SiO_2} * \mathrm{B_2O_3} \\
&\quad + b_{13}\mathrm{SiO_2} * \mathrm{Na_2O} + b_{23}\mathrm{B_2O_3} * \mathrm{Na_2O} + b_{14}\mathrm{SiO_2} * \mathrm{Al_2O_3} + b_{34}\mathrm{Na_2O} * \mathrm{Al_2O_3} + b_{15}\mathrm{SiO_2} * \mathrm{MgO}. \\
&\quad + b_{16}\mathrm{SiO_2} * \mathrm{Fines} + b_{17}\mathrm{SiO_2} * \mathrm{FP} \\
r(\mathrm{VRZ}) &= c_1\mathrm{SiO_2} + c_2\mathrm{Al_2O_3} + c_3\mathrm{CaO} + c_4\mathrm{TiO_2} + c_5\mathrm{Nd_2O_3} + c_6\mathrm{ZrO_2} + c_{13}\mathrm{SiO_2} * \mathrm{CaO} + c_{23}\mathrm{Al_2O_3} * \mathrm{CaO} \\
&\quad + c_{43}\mathrm{TiO_2} * \mathrm{CaO} + c_{12}\mathrm{SiO_2} * \mathrm{Al_2O_3} + c_{15}\mathrm{SiO_2} * \mathrm{Nd_2O_3}
\end{aligned}$$

For each domain, glass compositions were selected using NEMROD, a software tool capable of proposing the minimum number of points statistically required to build and then try to validate the postulated model.

Following this approach we fabricated 25 AVM glasses, 21 VRZ glasses and 25 R7T7 glasses; the center of gravity of each domain was included among the test compositions. The alteration rates of these glasses were determined by leaching experiments and the obtained results allowed us to determine the model coefficients $(a_1, a_2, \ldots, b_1, b_2, \ldots, c_1, c_2, \ldots)$.

Once the model has been established, the effect of a constituent on the alteration rate can be assessed on the whole composition domain. The results can the be plotted on a chart representing the effect of the variation of a constituent from the lower to the upper limit of its composition range, while the relative values of the other constituents remain at their center-of-gravity value. The percentage values express the weight of the constituent variation (upper limit − lower limit) with respect to the range of variations observed over the domain $(Y_{\max} - Y_{\min})$ [18]:

$$\frac{\text{Upper limit} - \text{lower limit}}{Y_{\max} - Y_{\min}}.$$

2.3. Experimental procedures

2.3.1. Testing under 'initial rate' conditions

The initial alteration rate in pure water at 100 °C (±0.5 °C) was determined using a Soxhlet device in compliance with the applicable French standard [25] on coupons polished to grade 4000 and washed; the shape of the test coupons allowed their surface area to be estimated simply and accurately [26] . Solution samples were taken at regular intervals (3, 7, 14, 28 days), acidified with 1 N HNO_3 and analyzed by ICP-AES (Si, B, Na, Li, Mo, Al, Ca). The uncertainty ranged from 3% to 5% depending on the elements considered.

2.3.2. Testing under 'saturation' conditions

The glass alteration kinetics at high reaction progress were studied by static leaching experiments at 50 °C for R7T7 and AVM glasses and 90 °C for VRZ glasses with the 63–125 μm powder size fraction; the S/V ratio was between 6000 and 7000 m^{-1}. Each 500 ml PTFE reactor was placed in a 1-l container with a few milliliters of water to limit evaporation. Solution samples were taken at regular intervals (7, 14, 28, 56, 91, 182, 364 days) from each reactor, ultrafiltered to 10 000 daltons, acidified with 1 N HNO_3, and analyzed by ICP-AES (Si, B, Na, Li, Cs, Al, Ca). The uncertainty ranged from 3% to 5% depending on the elements considered. The pH and temperature were measured for each sample with an ORION electrode.

Remarks: The glass alteration kinetics at high reaction progress were studied by experiments at 90 °C for VRZ glasses and not at 50 °C as for R7T7 and AVM glasses because measuring the alteration with accuracy at this temperature would have been difficult. It does not hinder comparison between the three composition domains. Indeed, alteration rates of VRZ glasses (measured at 90 °C) are smaller than alteration rates of R7T7 and AVM glasses (measured at 50 °C). It is not necessary to calculate alteration rates of VRZ glasses

at 50 °C according Arrhenius law to conclude that the alteration rate at high reaction progress of these glasses is clearly inferior to the alteration rates of the two other glasses.

2.3.3. SEM observations

The altered glass samples were observed with a scanning electron microscope. The altered glass coupons were cut at right angles to their largest surface, then embedded in resin. Polishing to within 1 μm revealed their alteration profile. The surface of the polished cross sections was covered with carbon or platinum prior to field-effect scanning electron microscope observation (JEOL 6330 with PGT analysis system). Platinum metallization was used to enhance the image quality at high magnification, and thus to measure very thin alteration depths. Coupling with an energy-dispersive (EDS) analyzer allowed element distribution maps to be plotted, making qualitative or semi-qualitative chemical analysis possible on the carbon-metallized specimens.

2.3.4. Results treatment

The results are expressed in terms of normalized mass loss for element (i) $NL_{(i)}$ or in terms of the equivalent alteration thickness $e_{(i)}$. $NL_{(i)}$ is calculated from the mass losses for element (i) normalized in terms to its mass fraction $x_{(i)}$ (grams (i)/unit mass of glass) in the unaltered glass and to the surface S in contact to the solution; $e_{(i)}$ corresponds to the glass thickness of density ρ altered to obtain the concentration $C_{(i)}$ in the solution volume V. The retention factor of an element in the alteration film is defined with respect to the elements dissolved congruently (boron, sodium and lithium for the tests described here).

Thus

$$NL_{(i)} = \frac{C_{(i)} \cdot V}{S \cdot x_{(i)}} \ (\mathrm{g\ m^{-2}}), \quad e_{(i)} = \frac{NL_{(i)}}{\rho} \ (\mathrm{m}),$$

$$\text{Retention factor}_{(i)} = 1 - \frac{NL_{(i)}}{NL(B, Na, Li)}.$$

3. Results

Table 2–4 list all the glass compositions studied and the results obtained for the three domains.

The initial alteration rate r_0 is calculated by linear regression from the normalized mass loss for boron NL(B) obtained during the Soxhlet tests with an accuracy of ±10%.

All the glass compositions were tested under static conditions at high S/V ratios (6000–7000 $\mathrm{m^{-1}}$) to investigate their kinetics at high reaction progress. The alteration rate for R7T7 and AVM glass at advanced stages of reaction progress r_f is determined by linear regression from the NL(B) values obtained for the last three samples (taken at 4 months, 6 months and 1 year). During alteration of VRZ glass samples at high S/V ratios at 90 °C, the normalized boron mass loss appear to be constant over time: the observed variations are not significant. It does not mean that r_f is zero but that r_f is too small to be measured with accuracy in these experimental conditions. We therefore considered the 1-year mean value r_{mean}(1 year) as being well expressed as the mean alteration rate estimated from $NL(B)_{mean}$:

$$r_{mean}(1\ \text{year}) = NL(B)_{mean}/360 \ (\mathrm{g\ m^{-2}\ d^{-1}}).$$

It considerably overestimates the alteration rate close to apparent saturation of the solution and r_{mean} is thus not directly comparable to r_f calculated for R7T7 and AVM glasses. However, it highlights the chemical durability of VRZ glasses at high reaction progress.

3.1. Initial alteration rate

Fig. 1 and Table 3 show the range of initial rates composition for each domain.

The initial alteration rates are relatively similar for glasses from all three domains, and in particular for the R7T7 and VRZ domains. The variation range is much greater within the AVM domain than for the R7T7 and VRZ domains.

From the experimental results, the software Nemrod allows to determine the coefficients of the postulated models to describe the variations of r_0 on each composition domain. The model corresponding to R7T7 domain is given as an example:

$$\begin{aligned} r_0(\mathrm{R7T7\ g\ m^{-2}\ d^{-1}}) = {} & 43.6SiO_2 + 189B_2O_3 + 30.5Na_2O \\ & + 15.2Al_2O_3 + 7.21Fe_2O_3 \\ & - 1.3\mathrm{Fines} - 43.4\mathrm{FP} - 447SiO_2 \\ & * B_2O_3 - 152SiO_2 * Na_2O \\ & + 115B_2O_3 * Na_2O - 81.1SiO_2 \\ & * Al_2O_3 - 186Na_2O * Al_2O_3 \\ & - 78.6SiO_2 * Fe_2O_3 - 73.3SiO_2 \\ & * \mathrm{Fines} - 19.7SiO_2 * \mathrm{FP} \end{aligned}$$

where each component is expressed as an oxide weight percentage in the glass with respect to the sum of the seven components. The other oxides ($CaO, Li_2O, \ldots$) are present in constant proportions, so the total differs from 100%). 'Fines' include platinum-group metals and metallic particles, FP refers to fission products.

The $r_0 = f(SiO_2, Al_2O_3, \ldots)$ models based on kinetic data are statistically validated by the software tool Nemrod over the entire range of glass compositions. This implies that there are no composition sub-ranges in which

Table 2
Glass compositions for experimentation plan and principal leaching results for R7T7 domain

R7T7 (oxide wt%)								Soxhlet	Testing under 'saturation' conditions				
No.	SiO_2	B_2O_3	Na_2O	Al_2O_3	Fe	F	FP	r_0 100 °C ($g\,m^{-2}\,d^{-1}$)	$pH_{50\,°C}$	$NL(B)_{1\,year}$ ($g\,m^{-2}$)	$NL(Si)_{1\,year}$ ($g\,m^{-2}$)	$C(Si)_{1\,year}$ ($mg\,l^{-1}$)	$r_{1\,year}$ ($g\,m^{-2}\,d^{-1}$)
1	42.4	12.4	8.1	6.6	5.6	0.01	15.4	1.94	8.9	0.05	0.014	17	5.9E–05
2	42.4	12.4	11.0	6.6	0.4	6.85	10.9	2.15	9.3	0.16	0.025	31	2.0E–04
3	42.4	14.1	11.0	6.6	5.6	0.01	10.8	2.94	9.4	0.20	0.031	34	1.6E–04
4	42.4	14.1	8.1	3.6	4.3	0.01	18.0	1.79	9.2	0.18	0.031	39	1.0E–04
5	49.5	16.5	8.1	3.6	0.4	0.01	12.4	1.58	9.1	0.31	0.042	64	1.5E–04
6	51.6	14.9	11.0	3.6	0.4	0.01	9.0	1.61	9.4	0.32	0.058	87	7.4E–05
7	51.7	14.9	8.1	6.6	0.4	0.01	8.8	1.82	8.8	0.15	0.028	40	1.9E–04
8	49.2	16.4	11.0	6.6	0.4	0.01	7.0	2.38	9.2	0.31	0.039	50	3.2E–04
9	51.7	14.9	8.1	3.6	5.2	0.01	7.0	2.43	9.0	0.21	0.039	59	1.0E–04
10	42.4	14.1	8.1	6.6	1.3	6.85	11.1	3.06	8.6	0.08	0.016	21	8.0E–05
11	43.2	14.4	11.0	3.6	0.4	0.01	18.0	1.62	9.5	0.38	0.055	66	8.8E–05
12	44.5	12.9	8.1	6.6	0.5	0.01	18.0	1.31	8.7	0.09	0.021	24	1.6E–04
13	43.8	12.7	11.0	3.6	5.5	0.01	13.9	2.42	9.5	0.25	0.044	53	9.5E–05
14	43.8	12.7	8.1	3.6	5.5	6.88	10.0	2.62	8.8	0.16	0.030	37	1.5E–04
15	51.7	16.5	11.0	3.7	0.4	3.60	3.6	2.34	9.3	0.35	0.052	90	1.8E–04
16	51.7	16.5	8.1	6.6	0.4	3.60	3.6	2.08	8.9	0.22	0.028	50	3.2E–04
17	42.6	14.1	11.0	3.6	5.6	6.77	6.9	4.14	9.4	0.34	0.046	53	1.6E–04
18	50.2	14.5	8.1	3.6	0.5	6.77	6.9	2.5	9.0	0.23	0.036	62	1.7E–04
19	47.5	15.8	8.1	6.6	5.5	3.50	3.5	3.32	8.7	0.12	0.024	34	1.8E–04
20	50.8	14.7	11.0	6.6	0.4	3.50	3.5	2.29	9.0	0.23	0.031	47	2.9E–04
21	49.1	14.2	11.0	3.6	5.6	3.50	3.5	3.35	9.3	0.27	0.046	66	1.6E–04
22	45.6	14.2	9.5	5.1	2.7	2.90	10.5	2.63	9.2	0.18	0.031	42	1.6E–04
V1	44.0	14.2	8.8	4.3	3.5	1.45	14.2	2.27	9.0	0.16	0.027	39	1.2E–04
V2	48.7	15.4	10.3	4.3	1.6	3.25	7.1	2.37	9.1	0.26	0.036	57	2.0E–04
V3a	45.5	14.0	9.8	4.9	1.3	3	12.2	ND	9.1	0.17	0.029	42	2.7E–05
V3b	45.5	14.0	9.8	4.9	1.3	3	12.2	ND	9.2	0.18	0.033	17	2.7E–05
V3c	45.5	14.0	9.8	4.9	1.3	3	12.2	ND	9.0	0.18	0.029	31	2.7E–05

ND: not determined.

Table 3
Glass compositions for experimentation plan and principal leaching results for AVM domain

AVM									Soxhlet	Testing under 'saturation' conditions				
No.	SiO_2	B_2O_3	Na_2O	Al_2O_3	MgO	F	P_2O_5	FP	r_0 100 °C ($g\,m^{-2}\,d^{-1}$)	$pH_{50\ °C}$	$NL(B)_{1\ year}$ ($g\,m^{-2}$)	$NL(Si)_{1\ year}$ ($g\,m^{-2}$)	$C(Si)_{1\ year}$ ($mg\,l^{-1}$)	r_f ($g\,m^{-2}\,d^{-1}$)
1	38.6	16.8	18.9	9.0	7.5	1.8	0	3.4	9.75	9.8	2.80	0.018	19	4.8E–03
2	41.5	16.0	18.8	12.5	2.5	1.8	1.7	1.2	4.13	9.2	0.32	0.017	18	6.7E–04
3	38.5	16.7	15.0	12.5	2.5	1.8	0	9.1	5.98	9.0	0.16	0.013	14	3.1E–04
4	38.6	16.8	18.8	9.0	2.7	0.0	0	10.2	6.54	9.9	1.36	0.019	20	3.2E–03
5	43.7	19.1	18.8	9.0	2.5	0.0	1.7	1.2	4.03	9.6	2.01	0.022	26	4.5E–03
6	44.6	19.5	15.5	9.0	3.8	1.8	0	1.8	3.84	9.3	2.77	0.012	15	6.3E–03
7	41.8	16.0	15.0	9.0	2.5	1.8	1.7	8.3	4.74	9.2	0.35	0.019	22	7.3E–04
8	42.0	16.0	15.0	9.0	7.5	0.0	0	6.6	5.43	9.6	0.61	0.019	22	1.6E–03
9	45.6	17.4	16.9	12.5	2.5	0.0	0	1.2	3.26	9.0	0.29	0.016	16	6.0E–04
10	38.7	16.8	15.1	12.6	6.0	0.0	1.708	5.2	8.86	9.2	0.08	0.011	12	1.4E–04
11	41.1	16.9	16.3	10.5	4.7	0.7	0.8	5.0	6.14	9.3	0.16	0.014	16	3.1E–04
12	38.5	16.0	15.0	12.5	2.5	0.0	1.7	9.9	5.55	8.8	0.16	0.014	14	1.7E–04
13	38.5	16.0	15.0	9.0	7.5	0.0	0	10.1	7.62	9.7	3.23	0.016	17	7.2E–03
14	46.0	19.5	15.8	9.0	2.5	0.0	1.65	1.6	2.79	9.3	0.93	0.024	29	2.0E–03
15	38.5	16.0	18.8	9.0	6.8	1.8	1.7	3.5	7.64	9.6	0.67	0.009	9	2.0E–03
16	40.1	17.6	15.0	9.0	2.5	0.0	1.7	10.2	6.07	9.2	0.30	0.019	20	6.2E–04
17	38.5	16.8	18.8	12.5	2.5	1.8	1.7	3.5	4.95	9.2	0.54	0.013	14	1.0E–03
18	46.0	17.5	15.8	9.0	2.5	1.8	1.7	1.8	1.32	9.2	0.54	0.023	29	1.1E–03
19	43.0	16.4	15.0	9.0	2.5	0.0	0	10.2	1.8	9.0	0.22	0.017	20	4.2E–04
20	46.0	17.5	18.8	9.0	3.2	0.0	0	1.6	2.89	9.8	1.49	0.022	27	3.4E–03
21	43.0	16.4	15.0	9.0	7.3	0.0	1.7	3.7	5.89	9.2	0.13	0.020	23	2.6E–04
22	38.5	16.0	18.8	12.5	6.1	0.0	0	4.2	7.03	9.4	0.16	0.012	13	3.5E–04
V1	39.9	16.9	17.7	9.7	3.6	0.3	0.4	7.6	6.28	9.6	0.45	0.018	20	1.1E–03
V2	42.5	18.0	17.7	9.7	3.6	0.3	1.2	3.1	4.99	9.4	0.56	0.018	21	1.3E–03
V3	43.4	17.1	16.7	11.5	3.6	0.3	0.4	3.1	4.39	9.2	0.28	0.016	16	6.1E–04

Table 4
Glass compositions for experimentation plan and principal leaching results for VRZ domain

VRZ								Soxhlet	Testing under 'saturation' conditions				
No.	SiO_2	Al_2O_3	CaO	TiO_2	ZrO_2	Nd_2O_3	B_2O_3	r_0 100 °C ($g\,m^{-2}\,d^{-1}$)	$pH_{90\,°C}$	$NL(B)_{mean}$ ($g\,m^{-2}$)	$NL(Si)_{1\,year}$ ($g\,m^{-2}$)	$C(Si)_{1\,year}$ ($mg\,l^{-1}$)	r_{mean} ($g\,m^{-2}\,d^{-1}$)
1	51.5	13.7	24.6	6.2	2.0	1.0	1	0.49	8.70	0.018	0.013	19	4.3E–05
2	55.6	9.0	19.7	6.2	2.0	6.5	1	0.78	8.67	0.019	0.019	38	5.6E–05
3	50.7	9.0	24.6	6.2	2.0	6.5	1	1.25	8.95	0.028	0.018	26	8.0E–05
4	41.8	9.0	19.7	15.5	12.0	1.0	1	0.79	8.51	0.017	0.013	18	4.4E–05
5	55.6	9.0	24.6	6.2	2.6	1.0	1	0.55	8.84	0.015	0.014	27	4.0E–05
6	40.8	13.7	24.6	6.2	7.2	6.5	1	1.74	8.85	0.027	0.012	14	8.0E–05
7	40.8	9.0	24.6	15.5	8.1	1.0	1	1.43	8.69	0.016	0.014	20	4.9E–05
8	40.8	9.0	19.7	11.0	12.0	6.5	1	1.03	8.55	0.017	0.014	19	5.4E–04
9	40.8	9.0	19.7	15.5	7.5	6.5	1	1.08	8.60	0.022	0.014	19	7.0E–05
10	41.6	13.7	19.7	15.5	7.5	1.0	1	0.98	8.42	0.017	0.012	16	4.5E–05
11	52.4	9.0	24.6	10.0	2.0	1.0	1	1.06	8.73	0.018	0.014	25	4.6E–05
12	55.6	9.0	19.7	10.9	2.9	1.0	1	0.97	8.54	0.015	0.017	38	4.9E–05
13	42.2	13.7	24.6	10.0	2.0	6.5	1	2.60	8.84	0.022	0.014	17	5.8E–05
14	40.8	13.7	24.6	13.5	5.5	1.0	1	1.54	8.69	0.015	0.0080	12	4.3E–05
15	40.8	9.0	24.6	13.1	5.1	6.5	1	2.07	8.93	0.023	0.011	13	6.0E–05
16	51.2	13.7	19.7	6.2	7.2	1.0	1	0.55	8.53	0.019	0.014	22	5.2E–05
17	41.4	9.0	24.6	11.0	12.0	1.0	1	1.64	8.89	0.021	0.014	18	5.7E–05
18	40.9	13.7	19.7	8.6	9.6	6.5	1	1.26	8.59	0.019	0.0077	11	5.0E–05
19	40.7	9.0	24.6	8.6	9.6	6.5	1	1.36	8.87	0.019	0.0085	12	5.3E–05
20	55.6	9.0	19.7	6.4	7.4	1.0	1	0.57	8.59	0.016	0.011	21	4.5E–05
21	46.9	11.1	21.9	10.1	6.4	2.7	1	1.06	8.74	0.019	0.013	20	4.7E–05

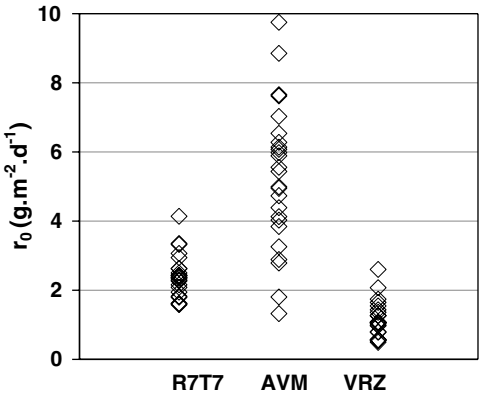

Fig. 1. Variability of the initial alteration rate measured at 100 °C within each domain.

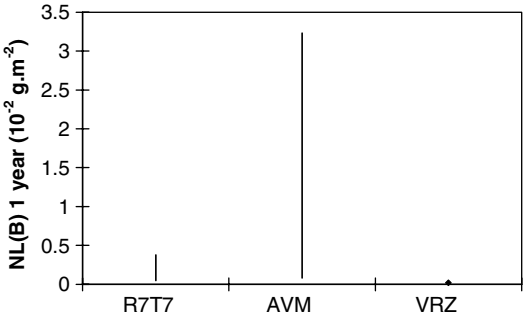

Fig. 2. Variability of normalized boron mass loss NL(B) ($g\,m^{-2}$) after 1 year measured at 50 °C for R7T7 and AVM domains and at 90 °C for VRZ domain.

the initial alteration rate is significantly different from the value calculated from the model.

The influence of a constituent ranging between its lower and upper composition limits, while all the other constituents ratios are unchanged at their center-of-gravity values, is indicated in Table 4: a minus sign indicates a reduction in the rate (by about 15% per sign) when the mass fraction of the constituent increases in the glass (from its lower to its upper limit).

Silica has a beneficial effect on the chemical durability of the material by diminishing the initial rate r_0. Conversely, increasing the concentrations of alkalis, alkaline earths and boron cause r_0 to increase.

The observed effect of the constituents is in agreement with other published work [1–3]. The Fe + Ni + Cr group slightly increases the initial alteration rate whereas the fission products, particularly the rare-earth elements and zirconium, improve the glass alteration resistance under initial rate conditions.

3.2. Alteration kinetics at advanced stages of reaction progress

Fig. 2 and Table 5 show the amplitude of the normalized mass loss variations after 1 year for each of the three composition domains.

The variability between domains is significantly greater than under initial rate conditions. This leads to very different kinetic profiles, as shown in Fig. 3.

The $r_f = f(SiO_2, Al_2O_3, B_2O_3, NaO, \ldots)$ models based on kinetic data having been statistically validated for the R7T7 and AVM domains (as for the model r_0), the effect of individual constituents can be determined. Table 6 summarizes the results obtained.

The variability of the VRZ glass alteration rates was very low (not exceeding a factor of 2), no effect of any constituent could be identified: under these conditions

Table 5
Variability of the initial alteration rate within each domain $r_{0\,max}$: maximum initial alteration rate; $r_{0\,min}$: minimum initial alteration rate

	$r_{0\,max}$ ($g\,m^{-2}\,d^{-1}$)	$r_{0\,min}$ ($g\,m^{-2}\,d^{-1}$)	$r_{0\,max}/r_{0\,min}$
R7T7	4.1	1.6	2.6
AVM	9.7	1.3	7.5
VRZ	2.6	0.49	5.3

the alteration rate is independent of the composition over the tested composition domain (Table 7).

3.3. Assessment of alteration kinetics

Although the three domains present relatively similar initial alteration rates, the variability of alteration rates among the domains increases with the reaction progress. The amplitude of the variations of normalized mass losses within each domain also increased (except for the VRZ domain). Nevertheless, the alteration kinetics of each domain present specific characteristics as shown by the following detailed results (Table 8).

Within the R7T7 domain, both the silicon concentration and the H_4SiO_4 activity varied almost as much as the boron concentration after 1 year. The silicon retention factor, however, was relatively independent of the composition but varied over time as shown in Fig. 4. The mean silicon retention increased from 66% after 7 days to 85% after 1 year of alteration. Silicon retention within the gel is considered to be one of the parameters affecting the protective properties of the gel layer [10].

For the AVM domain, the final rate calculated by linear regression over the last three sampling periods accounts for the entire altered thickness after 1 year as shown in Fig. 5.

The composition does not appear to have a significant effect on the normalized boron mass loss, and thus

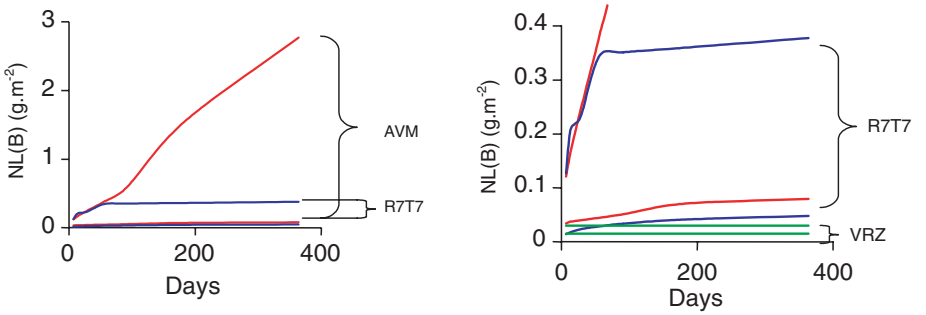

Fig. 3. Kinetic profiles for the three composition domains investigated: each domain is delimited by the kinetic profiles corresponding to the least and most altered glass samples. The left figure shows the AVM and R7T7 domains. The right figure is an expanded-scale view of the R7T7 and VRZ domains.

Table 6
Effect of constituents on the initial alteration rate (see text for details)

	SiO_2	Al_2O_3	B_2O_3	Na_2O	FP	Fe–Cr–Ni	Fines	MgO	F	P_2O_5	CaO	Nd_2O_3	ZrO_2	TiO_2
R7T7	–	+	++	+	–	++	+							
AVM	–	+	++	+	+			++	–	+				
VRZ	–	+									++	+	–	+

Table 7
Variability of normalized boron mass loss: NL(B) (g m^{-2}) after 1 year for each domain: $NL(B)_{max}$: maximum normalized mass loss; $NL(B)_{min}$: minimum normalized mass loss

	$NL(B)_{max}$ (g m^{-2})	$NL(B)_{min}$ (g m^{-2})	$NL(B)_{max}$/ $NL(B)_{min}$
R7T7	0.4	0.05	8
AVM	3	0.08	40
VRZ	0.03	0.015	2

on the alteration rate, within the VRZ domain. All the glasses studied exhibited a kinetic profile characteristic of an extremely low long-term alteration rate with constant boron mass losses over time (Fig. 6). The estimated decrease in the rate r_0/r_f exceeds a factor of 13000.

4. Discussion

Several hypotheses can account for the observed differences among the three glass composition domains. A pH variation could possibly explain the variable alteration of the glass. Moreover, the evolution of the kinetics over time can be due to a variation in the protectiveness of the alteration gel and possibly to the presence of secondary phases [10].

The $pH_{50\,°C}$ varied between 8.6 and 9.5 within the R7T7 domain and between 8.8 and 9.8 within the

Table 8
Summary table of constituent effects on long term leaching behavior (AVM, R7T7)

AVM			R7T7		
NL(B) and $r_{1\,year}$	$C(Si)_{1\,year}$		$r_{1\,year}$	$NL(B)_{1\,year}$	$C(Si)_{1\,year}$
–	+++	SiO_2	ns	–	++
–	–	Al_2O_3	++	–	–
+++	ns	B_2O_3	+	++	+
++	+	Na_2O	+	++	++
ns	ns	FP	–	–	–
Not tested	Not tested	Fe–Ni–Cr	–	–	–
Not tested	Not tested	Fines	ns	–	ns
+	–	MgO	Not tested	Not tested	ns
+	ns	F	Not tested	Not tested	–
–	+	P_2O_5	Not tested	Not tested	ns

ns: no significant effect.

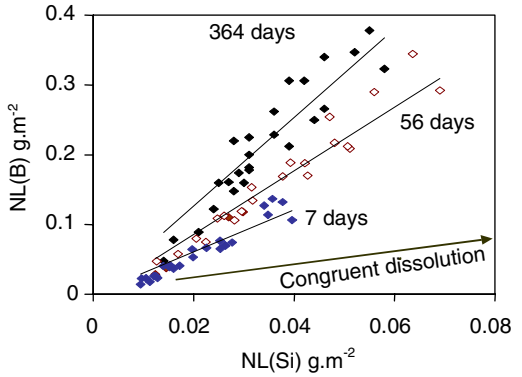

Fig. 4. NL(B) versus NL(Si) (g m^{-2}) for 57T7 glasses at three sampling intervals (7, 56 and 364 days) compared with congruent dissolution (NL(B) = NL(Si)). The normalized silicon mass loss is substantially lower than the normalized boron mass loss, indicating strong silicon retention within the alteration film. The NL(B)/NL(Si) ratio is constant at any given time interval and increases over time, i.e. the silicon retention factor increases over time.

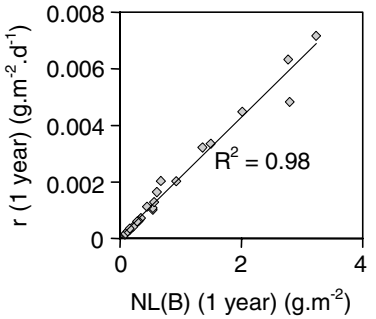

Fig. 5. One-year alteration rate (measured by linear regression over the last three sampling periods) versus NL(B).

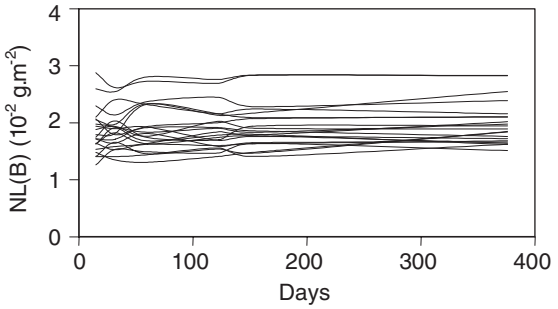

Fig. 6. Kinetic profile of VRZ glass during alteration at high S/V ratios at 90 °C.

AVM domain. Fig. 7 shows that the pH difference between the two domains is small compared with the differences between glasses within a single domain.

The $pH_{90\,°C}$ of the residual glass in the glass–ceramic varied from 8.3 to 8.8. If the hydroxide ion is considered the main cause of hydrolysis of the glass network in alkali media, comparing the pH for two different temperatures at constant OH^- activity shows that a pH of 8 at 90 °C is equivalent to a pH of 9 at 50 °C (pKe (50 °C) = 13.2; pKe (90 °C) = 12.4).

The rise of pH is not a direct cause of long-term R7T7 glass alteration in this pH range [18]. Indeed, several experiments have been carried out over 2 years with the SON68 reference glass (belonging to the R7T7 domain) at imposed pH values of 7, 8, 9.5, 10, 10.5, 11 and 11.5, in a closed system at 90 °C with an S/V ratio of 5000 m^{-1}. The results showed that in the pH range between 7 and 10 at 90 °C, the altered glass thickness after 1 year did not increase with the imposed pH, but instead decreased [14]. The pH measured in solution during these tests must therefore not be interpreted as a direct cause of R7T7 glass alteration.

Observation of the alteration films on AVM glass with a scanning electron microscope or even with the naked eye revealed very large quantities of crystallized secondary phases (Fig. 8).

After sieving and washing to separate the crystalline phases and glass grains, chemical analysis (by alkaline melting or dissolution in $HF/HNO_3/H_2SO_4$ and evaporation followed by dissolution in HCl/HNO_3 for ICP analysis), confirmed by X-ray diffraction measurements, showed phases highly enriched in magnesium with the following stoichiometry: $Si_3Al_1Mg_3$. Fig. 9 shows that the magnesium was entirely retained in the crystallized phases unlike the calcium, which contributed to the formation of the amorphous gel.

The crystallized phases consist of entangled filaments and did not adhere strongly to the glass. Unlike the gel, they cannot constitute a protective barrier against alteration. By consuming altered glass elements that could contribute to the construction of the gel (e.g. silicon and aluminum), the formation of crystallized phases enters into competition with the gel formation kinetics and limits the increase of element concentrations in solution. Such phases do not form during R7T7 and VRZ glass alteration because these glasses do not contain magnesium. Phyllosilicates rich in zinc and iron are observed on the surface of R7T7 glass, however, although these phases account for only a small fraction of the alteration film (about 5 wt% [12]), whereas a simplified calculation shows that the magnesia phase can represent up to 30 wt.% of the alteration film on AVM glass, as shown by SEM observations. Titanium-rich crystalline phases assumed to be phyllosilicates are also observed on the surface of VRZ glass. They are found in small quantities and have not yet been accurately identified.

If the formation of secondary phases accounts for a constant residual rate in AVM glass, can it be the same with R7T7 glass? No such phenomenon was observed in

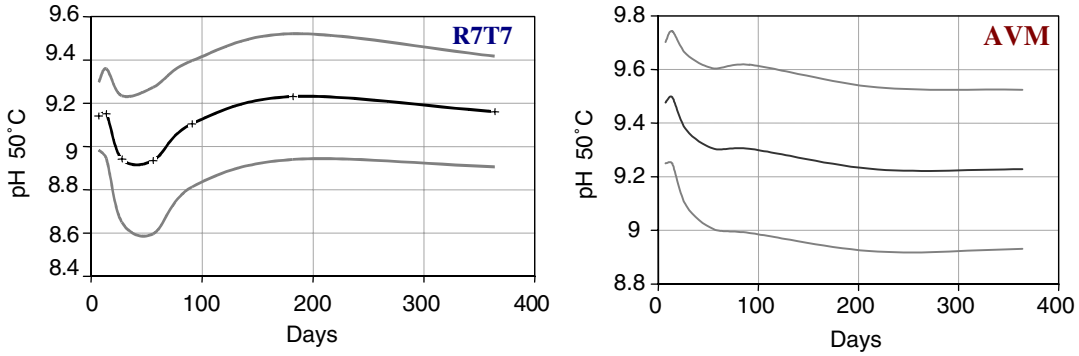

Fig. 7. Mean pH versus time for the R7T7 and AVM domains (± standard deviation due to change in the glass composition): mean pH (black), pH ± standard deviation (gray).

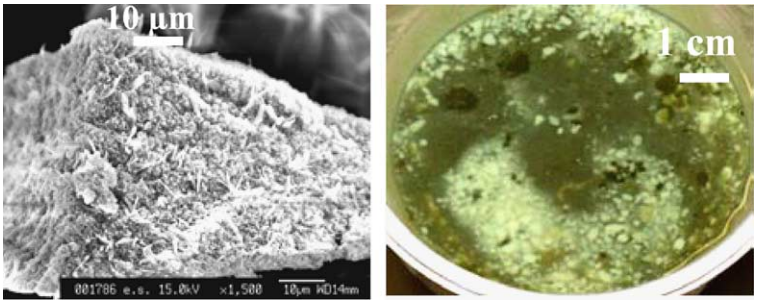

Fig. 8. Alteration film on the surface of an AVM glass: SEM image of an altered grain (left) and photo of the altered glass powder (right).

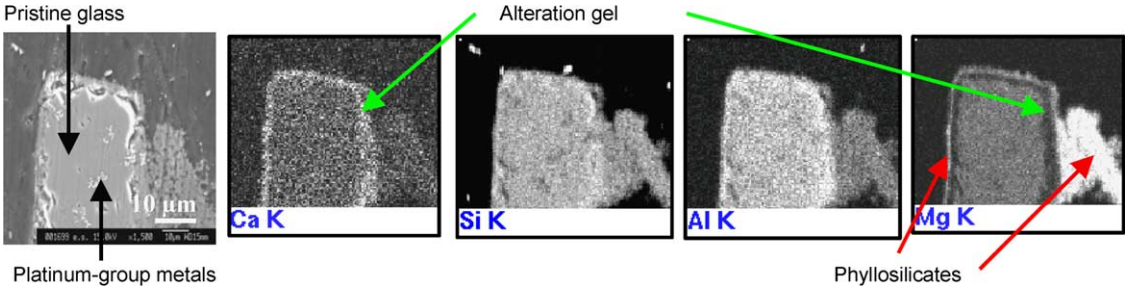

Fig. 9. SEM observations of the alteration film on AVM glass: element distributions.

the experiments discussed here. This is consistent with the fact that R7T7 glass contains no magnesium. Consequently, it leads to few secondary products that can not control silicon activity in the solution. However, under experimental conditions designed to obtain a more significant decrease in the alteration rate (higher temperatures and longer durations) Gin et al. found a very low residual alteration rate for R7T7 glass of about 10^{-4} g m^{-2} d^{-1} [14].

New data were provided by examining the effect of the constituents on measurable experimental parameters such as the 1-year alteration rates, the altered glass thicknesses, and the silicon concentration in solution.

The effect of the constituents on C(Si) for the VRZ domain is not discussed here; although the $C(\mathrm{Si}) = f(\mathrm{SiO_2}, \mathrm{CaO}, \mathrm{Al_2O_3}, \ldots)$ model is statistically valid, only SiO_2 has a significant coefficient value.

4.1. Silicon concentration in solution

The silicon concentration in solution C_{Si} is the result of the dynamic equilibrium between glass and solution: a

part of silicon coming from glass dissolution goes into solution and the other forms the alteration film (gel and secondary phases). Silicon concentration in solution is the result of these different processes: glass dissolution, alteration film formation and dissolution.

Within the R7T7 domain, the effect of the glass constituents on C_{Si} is the same as on the altered thickness: the same elements that enhance silicon recondensation also diminish the glass alterability. This observation confirms the formation of a protective gel and the fact that the silicon concentration is above all a measure of the reactivity of the gel rather than of the secondary phases. Silicon concentration ranges from 20 to 100 mg l^{-1} for a $pH_{50\,°C}$ around 9.1.

Within the AVM domain, the effect of the glass constituents on C_{Si} is very different from the effect on the altered thickness. This means that C_{Si} represents not only the dissolution–condensation dynamics of the potentially protective gel, but even more the dynamics of the secondary phases. Indeed, the higher the Mg and Al concentrations in the glass, the lower C_{Si}; adding magnesium in solution favors the formation secondary phases and thus consumes larger quantities of silicon in solution. Silicon concentration ranges from 10 to 30 mg l^{-1} for a $pH_{50\,°C}$ around 9.1 which is three times lower than R7T7.

4.2. Altered glass thickness after 1 year

The effect of the constituents is not the same as under initial rate conditions. As previously observed [1–3], aluminum favors the rapid development of a protective gel with a significant decrease in the rate during the initial instants of gel formation. The fines, which are rich in molybdenum (a relatively mobile element) and zirconium (a sparingly soluble structural element), have little effect on the glass containment properties. The fission products, rich in rare-earth elements and zirconium, improve the glass alteration resistance.

The link between the massive formation of secondary phases and sustained alteration is further strengthened by the observation that a high magnesium concentration increases the altered AVM glass thickness after 1 year. However, the undesirable effect of magnesium is not stronger than that of the alkali metals and boron. This suggests that the most pertinent parameter is not only the formation of the phases, but rather the kinetics of their formation compared with the kinetics of formation of the protective gel.

Several parameters could enhance the protectiveness and the kinetics of formation of a gel.

4.3. Affinity effect

If no secondary phases form, the element concentrations in solution (silicon in particular) will be higher, and will thus enhance the recondensation kinetics. At comparable pH values, the silicon concentrations are limited to about 30 mg l^{-1} for AVM glass, but may reach 100 mg l^{-1} for R7T7 glass.

4.4. Structure effect and element recondensation tendency

A strong synergy between calcium and aluminum, as well as between calcium and zirconium, has been demonstrated in the formation of a protective gel: at 90 °C and 8000 m^{-1}, the decrease in the alteration rate becomes significant when calcium and aluminum (or calcium and zirconium) are added to a three-oxide composition SiO_2–B_2O_3–Na_2O while maintaining the elemental ratios of R7T7 glass [13,8]. The high calcium, zirconium, aluminum, titanium and neodymium concentrations of VRZ glass favor silicon recondensation; the long-term Si concentration in solution remains about 30 mg l^{-1} at 90 °C. The decrease in the alteration rate is progressive for aluminum-rich glass (lower altered thickness, but higher 1-year rate), but occurs later and more suddenly for zirconium, the main fission product component (slightly lower altered thickness and major decrease in the 1-year rate). These results are comparable with the effects observed for simple glass compositions [10] (Fig. 10).

4.5. Porosity effects

The formation of a gel is not sufficient if it is not protective. This implies that the gel reorganization occurs quickly enough to fill-in the voids left by the release of the soluble elements, boron and alkali metals. For example, while an alkaline pH enhances the silica dissolution kinetics, as shown by alteration tests under initial rate conditions (i.e. with a high renewal rate), it may similarly enhance the recondensation kinetics in the gel and thus favor its reorganization [10].

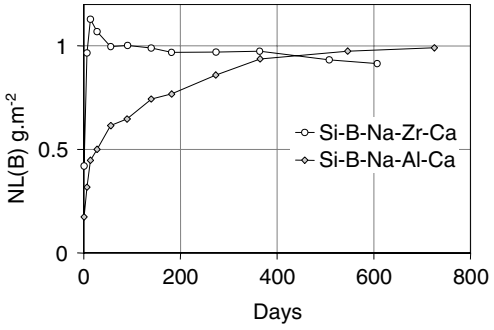

Fig. 10. Effect of Al and Zr on the alteration kinetics of simplified glasses to be compared with the effects of Al, and FP on $r_{1\,year}$ and $NL(B)_{1\,year}$ in the R7T7 domain (Table 8).

The mass fractions remaining after release of the elements that are not retained in the gel are very different depending on the composition domain. Over the long term, when steady-state concentrations are reached for the cross-linking elements in solution (near 100% retention) compared with the mobile tracer element, the mass fraction of elements remaining in the gel (glass composition less boron, alkali metals and crystallized secondary phases) is near 99% for VRZ glass, 70–80% for R7T7 glass, and only 47–64% for AVM glass.

5. Conclusion

The alteration characteristics of the glasses in the same composition domain are very comparable, making it a simple matter to apply predictions for the reference composition to the entire domain. The most significant differences in the alterability of the glass compositions appear in a closed system over long alteration periods; the altered thicknesses are particularly low for VRZ glass. The initial rate and especially the decrease in the rate determine the altered R7T7 and VRZ glass thicknesses after 1 year, whereas the residual alteration rate determines the altered AVM glass thickness. The persistence of a high residual rate for AVM glass is related to the massive formation of phyllosilicate phases rich in magnesium. The mechanism of formation of these phases competes with the formation of a protective gel, and has not yet been described in sufficient detail. The residual alteration kinetics observed for R7T7 glass by Gin suggest that the alteration of R7T7 and AVM glass could differ only for the relative values of the key parameters (the initial rate and residual rate) rather than for the alteration mechanisms themselves. The sensitivity of the glass and gel compositions to the presence of crystallized secondary phases is a major issue related to the more general problem of interaction with environmental materials capable of supplying elements liable to form secondary phases.

References

[1] G.F. Piepel, P. Hrma, S.O. Bates, M.J. Schweiger, D.E. Smith, Pacific Northwest Laboratory, Battelle, PNL 85-02, UC 721, 1993.
[2] I. Tovena, T. Advocat, D. Ghaleb, E. Vernaz, F. Larche, in: A. Barkatt, R.A. Van Konynenburg (Eds.), Scientific Basis for Nuclear Waste Management XIII, Materials Reserach Society, Pittsburgh, PA, 1994, p. 595.
[3] W.G. Ramsey, PhD thesis, Clemson University, UMI Nb 9602280, 1995
[4] P. Frugier, PhD thesis of the University of Montpellier, 1999.
[5] P. Aagaard, H.C. Helgeson, Am. J. Sci. 282 (1982) 237.
[6] B. Grambow, Mater. Res. Soc. Symp. Proc. 50 (1985) 15.
[7] T. Advocat, J.L. Crovisier, B. Fritz, E. Vernaz, in: V.M. Oversby, P.W. Brown (Eds.), Scientific Basis for Nuclear Waste Management XIII, Materials Reserach Society, Pittsburgh, PA, 1990, p. 241.
[8] C. Jégou, S. Gin, F. Larché, J. Nucl. Mater. 280 (2000) 216.
[9] Y. Linard, T. Advocat, C. Jegou, P. Richet, J. Non-Cryst. Solids 289 (2001) 135.
[10] S. Gin, Mater. Res. Soc. Symp. Proc. 663 (2000) 207.
[11] G. Berger et al., Geochim. Cosmochim. Acta 58 (22) (1994) 4875.
[12] N. Valle, J. Sterpenich, E. Deloule, G. Libourel, Geochim. Cosmochim. Acta (2001) 1.
[13] C. Jégou, S. Gin, E.Y. Vernaz, F. Larché, International Congress on Glass XVIII, The American Ceramic Society, 1998.
[14] S. Gin, C. Jégou, in: A.A. Balkema (Ed.), Water–Rock Interaction, vol. 1, Villasimius, Italy, 2001, p. 279.
[15] S. Ribet, S. Gin, J. Nucl. Mater. 324 (2004) 152.
[16] S. Fillet, University of Montpellier, 1987.
[17] J. Caurel, E. Vernaz, D. Beaufort, in: V.M. Oversby, P.W. Brown (Eds.), Scientific Basis for Nuclear Waste Management XIII Symposium, Materials Reserach Society, Pittsburgh, PA, USA, 1990, p. 309.
[18] P. Frugier, I. Ribet, T. Advocat, P. Frugier, I. Ribet, T. Advocat, in: Conference ICEM Bruges, 2001.
[19] C. Martin, Mater. Res. Soc. Symp. Proc. (2001) 713.
[20] C. Martin, PhD thesis of the University of Montpellier, 2002.
[21] P. Loiseau, D. Caurant, N. Baffier, L. Mazerolles, C. Fillet, Mater. Res. Soc. Symp. Proc. (2001) 179.
[22] P. Loiseau , PhD thesis of the University of Paris VI, 2001.
[23] J.A. Corbel, Designs, Models and the Analysis of Mixture Data, Wiley-Interscience, 1990.
[24] D. Mathieu, R. Phan-Tan-Luu, Plans d'expériences, applications à l'entreprise, Editions Technip, Paris, 1997.
[25] AFNOR, XP X 30-403, 1999.
[26] F. Delage, J.L. Dussossoy, Mater. Res. Soc. Symp. Proc. 212 (1991) 41.